RSC Advances

ROYAL SOCIETY OF CHEMISTRY

www.rsc.org/advances

RSC Advances

PAPER

S-layer based biomolecular imprinting

Eva M. Ladenhauf[a], Dietmar Pum[a], Daniel S. Wastl[a], Jose Luis Toca-Herrera[a], Nam V. H. Phan[b], Peter A. Lieberzeit[*b], and Uwe B. Sleytr[*a]

Received 00th January 20xx,
Accepted 00th January 20xx

DOI: 10.1039/x0xx00000x

www.rsc.org/

This work describes the development of molecularly imprinted polymer (MIP) thin films by using reassembled S-layer protein arrays as templates. Crystalline bacterial cell surface layer (S-layer) proteins are among the most abundant biopolymers on earth and form the outermost cell envelope component in a broad range of bacteria and archaea. The unique feature of S-layer based imprints is the crystalline character of the reassembled S-layer protein lattice leading to a precisely controllable periodicity of surface functional groups and topographical features. By determining the Young (elastic) modulus of the S-layer protein with respect to that of the polymer at its gel point, the feasibility of the S-layer based biomolecular imprinting was confirmed. After imprinting the polymer with an S-layer coated silicon stamp, the sensitivity of the imprints and their selectivity in relation to various other proteins were investigated by Quartz crystal microbalance (QCM) studies. Furtheron, Polycationic ferritin (PCF) was bound in dense packing on the S-layer and subsequently used for stamping. Successful rebinding of PCF proved that the S-layer lattice can be used as template for making imprints of densely packed and, probably, perfectly oriented biologically functional molecules, a concept that can in principle be extended to a wide range of other biomolecules (e.g. antibodies).

Introduction

Molecular imprinting is a well-established technology for generating two- or three-dimensional polymeric matrices for the highly specific detection of chemical or biological analytes. [1] Specificity is obtained by using suitable templates, such as chemical compounds or biomolecules. Self-assembly between these templates and suitable functional groups of the monomers used lead to polymer structures that do not only complement the shape of said species, but also lead to arranging the functional groups to complement those of the template. Although molecular imprinting was originally developed for detecting and selectively enriching small molecules from liquid matrices by bulk polymer beads, [2, 3] extension towards planar sensing layers for larger molecules has attracted substantial attention in the field of biosensor development in recent years. [1, 4, 5] Moreover, planar molecular imprinting mimics the fundamental principle of molecular recognition in nature by offering a bio-analogous surface for binding molecules or antibodies. It is the resulting high sensitivity and selectivity of the imprinted surface towards biomolecules combined with the relatively straightforward and cheap fabrication which make molecular imprinting to a key option in the development of novel (bio)analytical sensors, separation methods and purification techniques. The main benefit of a molecularly imprinted sensing layer is the higher robustness of the polymeric material compared to its biological counterpart. Despite all that, it should be possible to improve the performance of molecularly imprinted surfaces as binding matrices by ensuring perfectly dense packing of, both, topographical features as well as functional groups on the respective template surface. As a matter of fact, in this case the template used for making such high density molecular imprints must be an ordered array of (bio)molecules. In this context, the use of crystalline bacterial surface layer proteins (termed S-layer proteins) seems to be particularly attractive, since S-layer protein lattices have already proven their outstanding properties as affinity and binding matrices in biotechnological and biomedical devices. [6-8]

Crystalline bacterial cell surface layer (S-layer) proteins are among the most abundant biopolymers on earth and form the outermost cell envelope component in a broad range of bacteria and archaea (Fig.1). [6]

[a]*University of Natural Resources and Life Sciences, Vienna, Department of Nanobiotechnology, Institute of Biophysics, Muthgasse 11, A-1190 Vienna, Austria*
[b]*University of Vienna, Department of Analytical Chemistry, Währingerstraße 38, A-1090 Vienna, Austria*

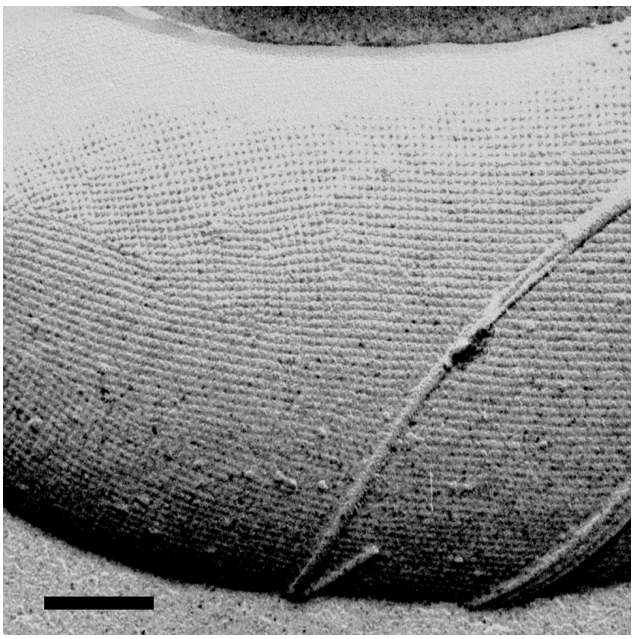

Fig.1 TEM micrograph of a freeze-etched and metal shadowed preparation of a bacterial cell of *Lysinibacillus sphaericus* with an S-layer as the outermost cell envelope component. The S-layer exhibits square (p4) lattice symmetry. The numerous lattice faults are a consequence of the bending of the S-layer lattice at the rounded cell poles. In addition, the rope-like structures are the flagella of the bacterial cell. Bar, 200 nm.

S-layer lattices consist of a single species of a protein or glycoprotein (M_w 40-200k Da) and may be considered the simplest biological membranes having developed during evolution. They are highly porous protein mesh works with pores of identical size (between 2 and 8 nm) and morphology. S-layers exhibit unit cell sizes of 3 to 30 nm and thicknesses of ca.10 nm. One of the key features of native and genetically modified S-layer proteins, including functionalized S-layer fusion proteins, [9, 10] is their natural capability to form self-assembled mono- or double layers in suspension, on solid supports, the air-water interface, planar lipid films, liposomes, nanocapsules, and nanoparticles (for review see references [6, 7, 11]).

This paper describes for the first time the use of S-layer protein lattices as templates in the fabrication of molecularly imprinted polymer surfaces following the scheme depicted in Fig.2. The unique feature of these imprints is the precisely controlled periodic repetition of topographical features and surface functional groups – induced by the crystalline character of the S-layer lattice. The application potential of such imprints will be great ranging from the development of bioanalytical sensors and affinity matrices to material science aspects where geometrically and surface chemically well defined arrays are required. The use of a bottom-up approach based on S-layer templated imprints in the formation of perfectly ordered arrays of metallic nanoparticles, carbon nanotubes, or biogenic silica and titania is new in the field. Current state of the art methods for self-assembly of nanoparticle arrays do not offer the control and flexibility of the S-layer approach but the spatial templating of these functional materials is essential to harnessing their superior optical and electronic properties for future devices. Furthermore, S-layers offer a rich structural palette. Namely, the two-dimensional lattice parameters can vary from species to species, allowing one to "tune" the desired lattice constant for a particular application. This is truly a remarkable property in a self-assembling system with the potential to transform large-area patterning without the use of limiting, i.e., expensive, standard lithographic processes. But, in addition to these more applied research aspects, it is anticipated that the binding of molecules similar in size, shape and surface functionalities which do not recrystallize by themselves could open new possibilities for elucidating their atomistic structure, e.g. by X-ray scattering techniques.

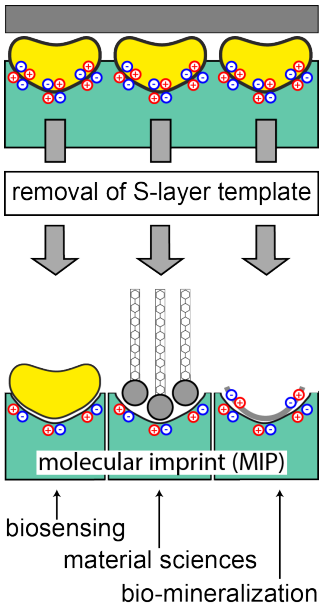

Fig.2 Schematic drawing of using S-layers as templates in molecular imprinting. Applications may range from the development of biosensors to scaffolds in material sciences, or as spatially controlled templates in bio-mineralization processes.

Experimental

Bacterial strains, growth conditions, cell wall preparations, and S-layer protein isolation

The S-layer proteins SbpA from *Lysinibacillus sphaericus* CCM2177 [12, 13] and SbsB from *Geobacillus stearothermophilus* PV72/p2 [14, 15] were used in this work.

L. sphaericus CCM2177 was grown in continuous culture nutrient broth medium under carbon limitation at 30°C [12, 13] and *G. stearothermophilus* PV72/p2 in SVIII medium at 57°C. Both organisms were harvested from the growth medium by centrifugation (at 10,000 g). Cell wall preparations of both S-layer proteins followed the procedures described previously. [16]

S-layer proteins were isolated from cell wall preparations by extraction with 5 M guanidine hydrochloride (GHCl; Fluka, Buchs, Switzerland) according to a previously described procedure. [16] The supernatant containing the proteins was dialyzed against 10 mM $CaCl_2$ (for SbpA) or milliQ water (for SbsB), respectively, as described previously. [16-18]

S-layer proteins

The S-layer protein SbpA of the bacterial strain *L. sphaericus* CCM2177 (equivalent to ATCC 4525 [19]) is currently one of the best-characterized S-layer proteins and often used in technological applications. [6, 12, 13, 20-23] Upon dialysis and addition of Ca^{++} ions [12, 13] SbpA assembles into ordered two-dimensional arrays with square

(p4) lattice symmetry in solution and at interfaces, including solid surfaces such as silicon, metals or polymers (for review see reference [11]). The size of the tetrameric unit cell is 13.1 x 13.1 nm, the thickness in the range of 8 to 9 nm. Calcium ions are mandatory for the reassembly process. [12, 24, 25] SbpA is non-glycosylated and shows a molecular weight of 129 kDa. With respect to the bacterial cell, the outer face is charge neutral due to an equal amount of free amino and carboxyl groups while the inner one is net positively charged due to an excess of amino groups. [26]

The SbsB S-layer protein with its molecular weight of 97 kDa is comparable in size to SbpA but reassembles in regular arrays showing oblique (p1) lattice symmetry with lattice parameters of a=10 nm, b=8 nm and a base angle of 81 °. The thickness of the S-layer lattice is approximately 4-5 nm. [27, 28] SbsB is non-glycosylated too. According to SbpA, the outer face is charge neutral but the inner face is net negatively charged due to an excess of free carboxyl groups. [27, 28]

Only SbpA S-layer protein lattices were used as templates in the imprinting process since these show pronounced surface corrugations and a thickness of 8-9 nm [22] while SbsB lattices are rather smooth and only 4-5 nm thick. [15, 29, 30]

Polymer synthesis and spin coating

Polymers were synthesized following protocols published in previous work. [31, 32] Best results were obtained using methacrylic acid (MAA) and vinylpyrrolidone (VP) in a ratio of 5:2 as functional monomers. The preparation started by mixing 180 μl MAA and 80 μl VP. In parallel and independent from each other, 17.5 mg N,N'-(1,2-dihydroxyethylene) bisacrylamide (DHEBA), which was used as cross-linker, were mixed with 600 ml dimetylsulfoxide (DMSO), and 500 mg sodium peroxide sulphate (SPDS) were mixed with 1 ml milliQ water. Subsequently, the entire DHEBA/DMSO solution, 7.8 μl of the MAA/VP solution, and 6.8 μl of the SPDS solution were mixed together and stirred in a water bath at a temperature of 68°C until the gel point was reached (typically after 12 min).

Stamp preparation

Silicon wafers were cut in 5 x 5 mm pads and pre-cleaned with 70 % ethanol and milliQ water. Very clean hydrophilic silicon surfaces were obtained after O_2 plasma treatment (20 s at 0.01 mbar) (Model Plasma Prep II, Gala Instruments, Germany). Subsequently, the silicon pads were placed on the surface of an S-layer protein solution (0.1 mg/ ml SbpA in 0.5 mm Tris-HCl buffer, pH 9, 10 mM $CaCl_2$, RT) in a beaker. The S-layer protein reassembled on the silicon surface and formed monolayers over night. [11, 33, 34]

For binding of polycationic ferritin (PCF) the reassembled S-layer proteins were treated with 2.5 % glutaraldehyde in 0.1 M Cacodylate buffer (pH 7.2) for 20 min to crosslink the amino groups. After washing with milliQ water for 5 min, PCF (Sigma life science; 10 mg/ mL) was bound to the free carboxyl groups (incubation time 10 min). [35-38]

Sensor fabrication and Quartz Crystal Microbalance (QCM) measurement

Dual-electrode sensor geometries (radius, 2.5 mm each) were screen-printed on AT-cut quartz discs (10 MHz, 15.5 mm in diameter, thickness 168 μm) with a brilliant gold paste (GGP 2093, 12%, Heraeus, Germany) and baked for 2 hrs at 400°C as published previously. [39] The screen was fabricated in a photolithographic procedure using a negative photoresist (Azocol Poly-Plus S, Kissel and Wolf, Wiesloch, Germany). A mask was used to transfer the electrode pattern into the photo resist by exposure to UV-light. While the exposed areas were hardened, the unexposed electrode structure could be removed by rinsing in warm water.

The quartz discs with the dual electrode configuration were spin-coated with the polymer subsequently. Thickness was typically in the range of 200 – 300 nm as determined by Quartz Crystal Microbalance (QCM) measurements. In the following, one electrode was imprinted and used as sensing electrode while the second one was not imprinted and served as (blank) reference. Imprinting was performed overnight at room temperature using the SbpA S-layer protein coated silicon pads as stamps. After careful removal of the stamp, the polymer coated quartz discs were placed in milliQ water for 1 hr and washed with 0,1 % sodium dodecyl sulfate (SDS), phosphate buffered saline (PBS) (10 mM, pH 7.4) and milliQ water in order to remove residual SbpA protein.

Sensors were investigated with a network analyser (Agilent 8712ETA, Agilent Santa Clara, CA) in a home-made measuring cell made of poly(dimethyl-siloxane) (PDMS; volume of 125 µL) at RT in liquid.[5] In the course of the measurements the analyte was injected into the cell and the mass uptake recorded for 7 min. In the following, between each measurement cycle, the measurement was paused and the sensor surface (imprinted and non-imprinted area) was washed for 15 min with 0.1 % SDS, PBS (10 mM, pH 7.4) and milliQ water in consecutive steps.

Determination of the Young modulus of the polymer at the gel-point

In order to determine the Young modulus of the polymer right after spin-coating (gel point), force-distance curves were recorded with an atomic force microscope (AFM) in due course. The Young modulus was calculated by the AFM software based on the Hertz model. The Hertz model approximates the sample as an isotropic and linear elastic solid. Furthermore, it is assumed that the intender – this is the AFM tip in our experiments – is not deformable and that there are no additional interactions between tip and sample. The latter assumption is accounted by using the extend curve only. Both, contact point and base line in a force indentation curve (tip – sample separation as x-axis, vertical deflection as y-axis) were fitted since it was very difficult to determine the real contact point due to the shallow angle of the curve around it. The Hertz model is valid for small indentations (5 - 10% of the total thickness). Therefore, the curve was fitted to an indentation between 3 nm and 16 nm because the thickness of the polymer layer was in the range of 200 – 300 nm and that of the S-layer approximately 8 nm. The individual spring constants of the cantilevers (Type DNP-S10, Bruker Metrology, k-values typically in the range of 0.06 N/m) were determined by the thermal noise method. [40] Moreover, a spherical tip with a radius of 100 nm (determined by scanning electron microscopy) and a Poisson ratio of 0.23 was assumed for the fitting procedure.

Atomic force microscopy

Imprinted and non-imprinted areas were investigated by atomic force microscopy (AFM) in contact and non-contact mode in buffer and also in air (Nanowizard I, JPK Berlin, Germany and Nanoscope V, Veeco, Santa Barbara, CA). [34, 41, 42] Non-conductive silicon nitride cantilevers (Type DNP-S10, Bruker Metrology) were used in both microscopes.

Results and discussion

Since the S-layer based imprinting approach is completely new in the field of molecular imprinting, in a first step, we assessed the Young (elastic) modulus (E) of the reassembled S-layer protein layer with respect to that of the polymer (oligomer film) at the gel-point (right after spin-coating). Only when the S-layer is stiffer than the polymer at the gel point, topographical features can be transferred from the S-layer lattice into the polymer. The Young modulus of the polymer at the gel-point was found to be 0.17 MPa. The compressibility (bulk) modulus of the S-layer protein SbpA is known to be 0.6-0.8 MPa corresponding to a Young modulus of 1.31 MPa. [43] The seven to eight times higher Young modulus of the S-layer with respect to that of the polymer led us to the conclusion that it must be possible to transfer the topography and pattern of functional groups of the S-layer protein lattice into the polymer.

After removal of the stamp and cleaning the molecularly (termed MIP) and non-molecularly imprinted polymer (termed NIP) areas, the sensitivity and selectivity of the MIP compared to those of the NIP were determined by exposing both areas to SbpA S-layer protein solutions (SbpA assemblies were used as templates during imprinting). QCM studies unambiguously demonstrated successful rebinding on the electrode surface (Fig. 3). Injection of 200 ppm (1 ppm= 1 mg/L) SbpA led to a frequency difference between MIP and NIP in the range of 400 Hz. The baseline refers to water. As shown in Figure 3 the S-layer protein also binds to some extent to the NIP since S-layer proteins bind to polymeric surfaces as well [11] but the MIPs are highly preferred. This experiment was repeated several times with a washing step between each measurement. Moreover, the rebinding experiments were carried out without calcium in the solution. Calcium ions are required for the reassembly of SbpA into ordered arrays. [12, 24, 25] The lack of calcium in the subphase guaranteed that only the rebinding of the SbpA proteins was measured and a possible lattice formation at the MIP or NIP avoided.

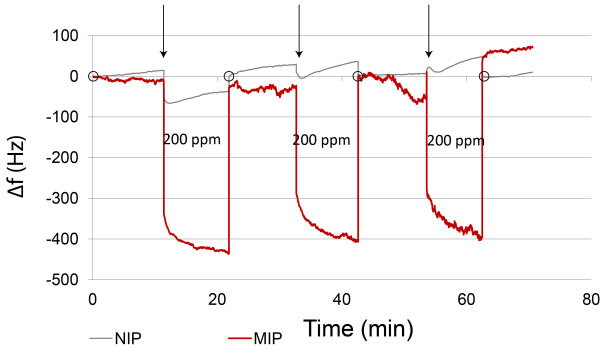

Fig.3 Diagram shows three repeats of rebinding S-layer protein (200ppm/ H_2O) on the molecularly imprinted surface. Measurement was paused during cleaning (injection of SDS-PBS and milliQ water). Baseline refers to water. Open circles (o) mark the start of a new measurement. At the start of a new measurement the first data value of the NIP signal was taken to correct an offset from the baseline caused by residual material after the cleaning step. Arrows indicate the addition of SbpA S-layer protein.

In a next step we determined the QCM sensor characteristic of the S-layer protein MIP and found it to be linear as shown in Figure 4. In the course of these experiments it turned out that the suitable concentration range for rebinding SbpA is 30 to 200 ppm. Above 200 ppm SbpA saturation starts to occur which corresponds to ca. 100 ng bound SbpA on the electrode surface (radius, 2.5 mm) (data not shown).

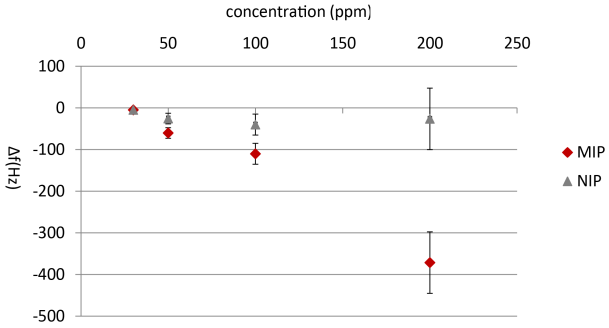

Fig.4 Diagram showing the linear relationship between the QCM frequency response and the S-layer protein concentration in the rebinding experiments. Data were obtained from individually prepared sensors.

Selectivity is another important aspect when characterizing a MIP. Therefore we exposed the SbpA MIP and NIP to solutions containing 200ppm other molecules, which are similar in size, namely another S-layer protein (SbsB, the S-Layer protein from *G. stearothermophilus* PV72/p2 in the concrete case) as well as Bovine Serum Albumine (BSA) (Fig.5).

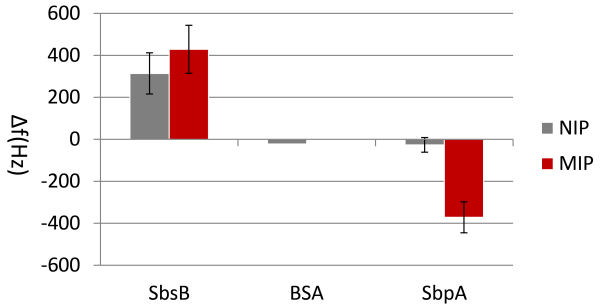

Fig.5 Diagram showing that no cross-selectivity to BSA and even an "Anti-Sauerbrey"- effect upon rebinding of SbsB is observed. As expected, SbpA binds preferentially to its own MIP. Data were obtained from individually prepared sensors.

While BSA does not lead to a response on the SbpA-MIP, the experiment with SbsB even led to an increase in frequency, a phenomenon that is known as Anti-Sauerbrey behaviour. This behaviour has already been observed in other QCM studies with proteins in the literature. [31, 32, 44] An increase in frequency may be caused by a weak binding of the analyte indicating a low affinity to the imprinted surface, for example when the molecules do not perfectly fit in the cavities of the imprint. [39] Thus, we assume that SbsB is only loosely bound and does not oscillate synchronously with the microbalance. After cleaning and rinsing the sensors with de-ionized water the initial frequency values of the baseline were obtained again. Moreover, it has to be noted that, contrary to SbpA, also the NIP shows an Anti-Sauerbrey behavior. We assume that SbsB forms monolayers in solution and those sheets that are close or attached to the MIP and the NIP are responsible for the observed phenomenon. It is likely, that such "rigid" molecular thin films affect the transverse motion of the sensor surface due to their moments of inertia more severely than single molecules. [45]

Atomic force microscopy (AFM) imaging of imprinted areas

AFM images of SbpA S-layer lattices reassembled on the stamp and of a molecular imprint are shown in Figure 6. However, despite the

initial assumption, it was very difficult to resolve the imprinted S-layer lattice at the MIP by AFM (contact and non-contact mode). It was only possible to see patterns in the S-layer imprint in the AFM error-deflection mode (Fig.6b). The S-layer imprinted lattice structure was confirmed by calculating the Fourier spectrum and analysing the reciprocal lattice. The first order spots, which indicate a lattice spacing of ca. 13 nm, are marked in the insets in Figure 6. We assume that several factors are responsible for this: (i) First of all, AFM of S-layer imprints is challenging considering that the mean depth of the S-layer protein induced cavities is approximately 3 to 4 nm while the average level of the corrugations of the polymer is between 200 and 300 nm. Thus, the signal level compared to the background variation is only in the 1% range. In this context, also plastic deformations, which have shown to occur also at extreme cryogenic temperatures (4K), may be considered.[46-48] (ii) Moreover, in case the polymer does not absorb the residual water contained in the pores and cavities of the S-layer protein lattice, a "deep" imprint of the S-layer in the polymer will not be possible since the S-layer will be squeezed by the water film and just the upper part of the protein lattice may contribute to the imprint. This hypothesis was supported by the observation that QCM data could not be obtained from the same polymer composition when water was used as solvent instead of DMSO. (iii) Finally, it was found that the polymer was swelling in liquid (milliQ water) within 20 min. But, high resolution AFM usually requires imaging in buffer in order to minimize the loading forces, in particular electrostatic interactions between tip and surface. However, AFM in air was used too in order to avoid the negative swelling effect but molecularly resolved S-layer structures were extremely difficult to obtain still.

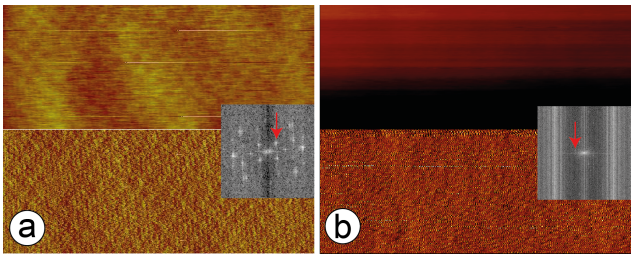

Fig.6 AFM images (contact mode in liquid) of (a) an SbpA monolayer on a silicon wafer used for stamping, and (b) an SbpA based molecular imprint. Height image (upper part; z-range 3 nm), deflection error image (lower part; z-range 0.3 nm), image sizes 300 x 120 nm. The insets show the corresponding Fourier spectra of the deflection error images. The first order spots are marked by red arrows.

Imprinting of PCF labelled S-layer proteins

Polycationic ferritin (PCF) is a ferritin molecule cationized by N,N-dimethyl-1,3-propanediamine (DMPA) with amino groups. PCF is a well-known marker molecule in transmission electron microscopy since the iron core yields high contrast and the positive charge allows the labelling of negatively charged groups, such as carboxyl groups, for example on proteins.[35, 37, 49, 50] PCF has a mean diameter of 12 nm, and thus is perfectly suited to label S-layer unit cells individually. The binding of PCF onto the S-layer and the subsequent molecular imprinting was done in order to show that it is possible to use the S-layer itself as a "stencil" for (bio)molecules, i.e to achieve optimal assembly, and to answer the question if the MIP still preferably rebinds PCF because the NIP offers free carboxyl groups on its surface too. In detail, does the imprinting of the positively charged PCF lead to a noticeable re-distribution of the carboxyl groups in the polymer into clusters of negative charge in addition to the topographical effect of a nano metric "egg carton" with hemi-spherical indentations in the 12 nm range. The rebinding of 200 ppm PCF led to an average frequency decrease of 450 Hz at the MIP and of 350 Hz at the NIP corresponding to a usable sensor signal of 100 Hz (Fig.7a).

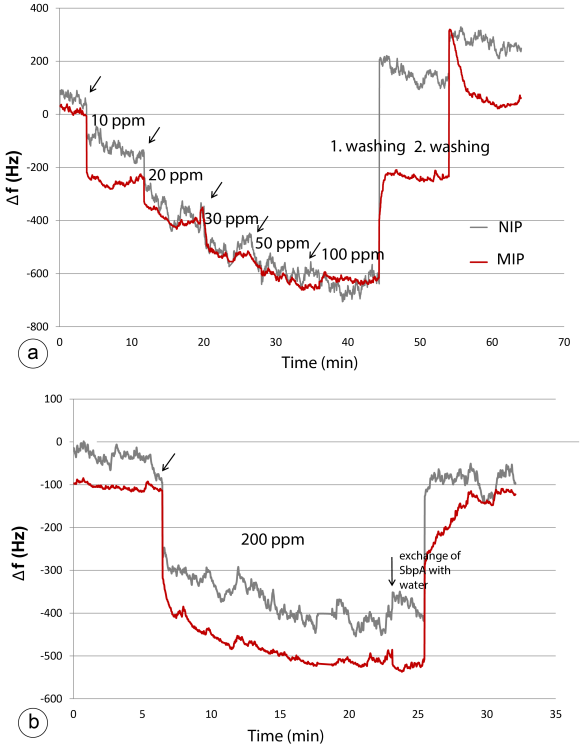

Fig.7 Diagram showing (a) the rebinding of PCF 200 ppm on imprinted and non-imprinted electrode surfaces. (b) PCF bound to the imprinted surfaces withstands the washing with SDS-PBS much better than that on the non-imprinted area. Baselines refer to water.

According to the investigation with the SbpA S-layer protein, the maximum amount of PCF that can be rebound to the imprinted area was also determined (Fig.7b). After addition of 10 ppm PCF, the frequency at the MIP decreased by 300 Hz while at the NIP by 200 Hz. After further additions of PCF leading to a (final) concentration of 50 ppm PCF in the analyte the saturation condition was reached. This was concluded from the observation that a further addition of 50 ppm PCF (leading to a final concentration of 100 ppm PCF in the analyte) did not lead to a further frequency decrease.

The positive effect of molecular imprinting for binding PCF could be demonstrated by washing the two PCF loaded sensor surfaces in two consecutive steps (Fig.7b). After the first washing step (10 min with 0.01 % SDS, PBS, and milliQ water, respectively) the electrode signal at the NIP reached the baseline again whereas the signal at the MIP did not change as much. In a second washing step (now 15 min) PCF that was still bound to the imprinted surface was removed as well. Moreover, the exchange of the analyte solution with water (marked by an arrow in Fig. 7a) did not lead to an increase of the MIP signal again.

Conclusions

The use of S-layer protein lattices is completely new in the field of molecular imprinting. It is the two-dimensional lattice, which make this approach so unique, because up to our knowledge, there is no other biological model system available which provides such a precisely controlled spatial distribution and orientation of physicochemical properties in the nano meter range. This feature of S-layer protein lattices has already been widely used in nanobiotechnological applications where molecules (e.g. enzymes, antibodies, ligands) or nanoparticles were bound into regular arrays such as in the development of high density affinity matrices [6-9, 30, 51, 52]. Moreover, with the design and expression of functional S-layer fusion proteins a new horizon in biotechnological and biomedical research was opened since then it was possible to specifically functionalize the S-layer proteins and thus the entire reassembled S-layer lattice. In this way, the molecular imprinting of S-layer proteins may become extremely valuable when functional domains such as streptavidin or metal precipitating peptides are fused with the S-layer proteins and imprinted into the polymeric surface. The proof-of-concept for this fundamental concept was shown here by binding PCF to the S-layer protein template in dense packing, imprinting the PCF array, and, after washing, rebinding PCF. Although the S-layer will only serve as a template and together with the functional layer sacrificed after the imprinting process, the molecularly imprinted sensing layer will be mechanically much more robust than its natural counterpart. Moreover, it might be possible but also extremely challenging to make a functional imprint of the imprint and in this way a "synthetic copy" of the topography and surface functional groups (or domains) of the original S-layer lattice. This approach would be a contribution to the rapidly growing area of synthetic biology, too. Moreover, a broad range of S-layer protein is glycosylated. [6, 53, 54] The carbohydrate chains are located at the outer S-layer face and – when the S-layer protein reassembles with its inner face at the stamp surface - thus accessible for molecular imprinting too. It would be interesting to see whether it is possible to bind and align carbohydrate chains in a precisely controlled way on a polymeric surface.

In summary, we would like to anticipate that our approach provides a key enabling technology for the fabrication of nano patterned molecular imprints by using self-assembling strategies common in nature. Application will be found in the life and non-life sciences wherever well defined repetitive topographic and (bio)chemical features in the nanometer range are required.

Acknowledgements

Part of this work was funded by AFOSR Agreement Awards Nr. FA9550-09-0342 and FA9550-12-1-0274 (to DP), and FA9550-10-1-0223 (to UBS), and by the Erwin-Schrödinger Society for Nanosciences, Vienna.

Notes and references

1. N. W. Turner, C. W. Jeans, K. R. Brain, C. J. Allender, V. Hlady and D. W. Britt, *Biotechnol Prog*, 2006, **22**, 1474-1489.
2. M. Glad, O. Norrlˆw, B. Sellergren, N. Siegbahn and K. Mosbach, *Journal of Chromatography A*, 1985, **347**, 11-23.
3. R. Arshady and K. Mosbach, *Die Makromolekulare Chemie*, 1981, **182**, 687-692.
4. F. L. Dickert and O. Hayden, *Anal Chem*, 2002, **74**, 1302-1306.
5. O. Hayden and F. L. Dickert, *Adv Mater*, 2001, **13**, 1480-1483.
6. U. B. Sleytr, B. Schuster, E. M. Egelseer and D. Pum, *FEMS Microbiol Rev*, 2014, **38**, 823-864.
7. E. M. Egelseer, N. Ilk, D. Pum, P. Messner, C. Schäffer, B. Schuster and U. B. Sleytr, in *Encyclopedia of industrial biotechnology: bioprocess, bioseparation, and cell technology*, ed. M. C. Flickinger, John Wiley and Sons, Hoboken, N.J., 2010, vol. 7, pp. 4424-4448.
8. U. B. Sleytr, P. Messner, D. Pum and M. Sára, *Angew. Chem. Int. Ed.*, 1999, **38**, 1035-1054.
9. N. Ilk, E. M. Egelseer and U. B. Sleytr, *Curr. Opin. Biotechnol.*, 2011, **22**, 824-831.
10. N. Ilk, E. M. Egelseer, J. Ferner-Ortner, S. Küpcü, D. Pum, B. Schuster and U. B. Sleytr, *Coll. Surf. A*, 2008, **321**, 163-167.
11. D. Pum and U. B. Sleytr, *Nanotechnology*, 2014, **25**, 312001.
12. D. Pum and U. B. Sleytr, *Thin Solid Films*, 1994, **244**, 882-886.
13. N. Ilk, C. Völlenkle, E. M. Egelseer, A. Breitwieser, U. B. Sleytr and M. Sára, *Appl. Environ. Microbiol.*, 2002, **68**, 3251-3260.
14. M. Sára, B. Kuen, H. F. Mayer, F. Mandl, K. C. Schuster and U. B. Sleytr, *J Bacteriol*, 1996, **178**, 2108-2117.
15. E. Baranova, R. Fronzes, A. Garcia-Pino, N. Van Gerven, D Papapostolou, G. Pehau-Arnaudet, E. Pardon, J. Steyaert, S. Howorka and H. Remaut, *Nature*, 2012, **487**, 119-122.
16. U. B. Sleytr, M. Sára, Z. Küpcü and P. Messner, *Archives of Microbiology*, 1986, **146**, 19-24.
17. N. Ilk, P. Kosma, M. Puchberger, E. M. Egelseer, H. F. Mayer, U. B. Sleytr and M. Sára, *J. Bacteriol.*, 1999, **181**, 7643-7646.
18. E. Egelseer, K. Leitner, M. Jarosch, C. Hotzy, S. Zayni, U. B. Sleytr and M. Sára, *J Bacteriol*, 1998, **180**, 1488-1495.
19. T. Pavkov-Keller, S. Howorka and W. Keller, *Prog. Molec. Biol. Transl. Sci.*, 2011, **103**, 73-130.
20. S. Chung, S. H. Shin, C. R. Bertozzi and J. J. De Yoreo, *Proc. Natl. Acad. Sci. USA*, 2010, **107**, 16536-16541.
21. S. H. Shin, S. Chung, B. Sanii, L. R. Comolli, C. R. Bertozzi and J. J. De Yoreo, *Proc. Natl. Acad. Sci. USA*, 2012, **109**, 12968-12973.
22. C. Horejs, H. Gollner, H. Pum, U. B. Sleytr, H. Peterlik, A. Jungbauer and R. Tscheliessnig, *ACS Nano*, 2011, **5**, 2288-2297.
23. J. E. Norville, D. F. Kelly, T. F. Knight, A. M. Belcher and T. Walz, *J. Struct. Biol.*, 2007, **160**, 313-323.
24. D. Pum and U. B. Sleytr, *Coll. Surf. A*, 1995, **102**, 99-104.
25. B. Rad, T. K. Haxton, A. Shon, S. H. Shin, S. Whitelam and C. M. Ajo-Franklin, *ACS Nano*, 2015, **9**, 180-190.
26. E. Györvary, A. Schroedter, D. V. Talapin, H. Weller, D. Pum and U. B. Sleytr, *J. Nanosci. Nanotech.*, 2004, **4**, 115-120.
27. D. Rünzler, C. Huber, D. Moll, G. Kohler and M. Sara, *The Journal of biological chemistry*, 2004, **279**, 5207-5215.
28. M. Sára, C. Dekitsch, H. F. Mayer, E. M. Egelseer and U. B. Sleytr, *J. Bacteriol.*, 1998, **180**, 4146-4153.
29. C. Horejs, D. Pum, U. B. Sleytr and R. Tscheliessnig, *J. Chem. Phys.*, 2008, **128**, 65106.
30. D. Moll, C. Huber, B. Schlegel, D. Pum, U. B. Sleytr and M Sára, *Proc. Natl. Acad. Sci. USA*, 2002, **99**, 14646-14651.

31. T. Wangchareansak, C. Sangma, K. Choowongkomon, F. Dickert and P. Lieberzeit, *Anal Bioanal Chem*, 2011, **400**, 2499-2506.
32. R. Schirhagl, P. A. Lieberzeit and F. L. Dickert, *Adv Mater*, 2010, **22**, 1992-1992.
33. D. Pum, G. Stangl, C. Sponer, W. Fallmann and U. B. Sleytr, *Coll. Surf. B*, 1997, **8**, 157-162.
34. E. S. Györvary, O. Stein, D. Pum and U. B. Sleytr, *J. Microsc.*, 2003, **212**, 300-306.
35. P. Messner, D. Pum, M. Sára, K. O. Stetter and U. B. Sleytr, *J. Bacteriol.*, 1986, **166**, 1046-1054.
36. D. Danon, Skutelsk.E, Marikovs.Y and Goldstei.L, *J Ultra Mol Struct R*, 1972, **38**, 500-510.
37. D. Pum, M. Sára and U. B. Sleytr, *J. Bacteriol.*, 1989, **171**, 5296-5303.
38. M. Sára and U. B. Sleytr, *J. Bacteriol.*, 1987, **169**, 2804-2809.
39. F. L. Dickert, O. Hayden, R. Bindeus, K. J. Mann, D. Blaas and E. Waigmann, *Anal Bioanal Chem*, 2004, **378**, 1929-1934.
40. J. L. Hutter and J. Bechhoefer, *Rev Sci Instrum*, 1993, **64**, 1868-1873.
41. D. Pum, J. Tang, P. Hinterdorfer, J. L. Toca-Herrera and U. B. Sleytr, in *Biomimetic and bioinspired nanomaterials*, ed. C. Kumar, Wiley-VCH, Weinheim, 2010, vol. 7, pp. 459-510.
42. D. Pum and U. B. Sleytr, *Supramol. Sci.*, 1995, **2**, 193-197.
43. A. Martín-Molina, S. Moreno-Flores, E. Perez, D. Pum, U. B. Sleytr and J. L. Toca-Herrera, *Biophys. J.*, 2006, **90**, 1821-1829.
44. U. Latif, S. Can, O. Hayden, P. Grillberger and F. L. Dickert, *Sensor Actuat B-Chem*, 2013, **176**, 825-830.
45. M. Rodahl and B. Kasemo, *Sensor Actuat a-Phys*, 1996, **54**, 448-456.
46. U. B. Sleytr and W. Umrath, *J Microsc-Oxford*, 1974, **101**, 177-186.
47. U. B. Sleytr and A. W. Robards, *J Microsc-Oxford*, 1982, **126**, 101-122.
48. U. B. Sleytr and A. W. Robards, *J Microsc-Oxford*, 1977, **110**, 1-25.
49. M. Sára, D. Pum and U. B. Sleytr, *J. Bacteriol.*, 1992, **174**, 3487-3493.
50. M. Sára and U. B. Sleytr, *J. Bacteriol.*, 1993, **175**, 2248-2254.
51. H. Tschiggerl, J. L. Casey, K. Parisi, M. Foley and U. B. Sleytr, *Bioconj. Chem.*, 2008, **19**, 860-865.
52. D. Pum and U. B. Sleytr, in *Nanobioelectronics - for electronics, biology, and medicine*, eds. A. Offenhäuser and R. Rinaldi, Springer, New York, 2009, DOI: Vch 2062, pp. 167-180.
53. P. Messner, C. Schaffer and P. Kosma, *Advances in carbohydrate chemistry and biochemistry*, 2013, **69**, 209-272.
54. B. Schuster and U. B. Sleytr, *Acta Biomater*, 2015, **19**, 149-157.